

11. Nijhawan, D. *et al.* Elimination of Mcl-1 is required for the initiation of apoptosis following ultraviolet irradiation. *Genes Dev.* **17**, 1475–1486 (2003).
12. Rinkenberger, J. L., Horning, S., Klocke, B., Roth, K. & Korsmeyer, S. J. Mcl-1 deficiency results in peri-implantation embryonic lethality. *Genes Dev.* **14**, 23–27 (2000).
13. Wei, M. C. *et al.* Proapoptotic BAX and BAK: a requisite gateway to mitochondrial dysfunction and death. *Science* **292**, 727–730 (2001).
14. Cheng, E. H. *et al.* BCL-2, BCL-X_L sequester BH3 domain-only molecules preventing BAX- and BAK-mediated mitochondrial apoptosis. *Mol. Cell* **8**, 705–711 (2001).
15. Letai, A. *et al.* Distinct BH3 domains either sensitize or activate mitochondrial apoptosis, serving as prototype cancer therapeutics. *Cancer Cell* **2**, 183–192 (2002).
16. Veis, D. J., Sorenson, C. M., Shutter, J. R. & Korsmeyer, S. J. Bcl-2-deficient mice demonstrate fulminant lymphoid apoptosis, polycystic kidneys, and hypopigmented hair. *Cell* **75**, 229–240 (1993).
17. Motoyama, N. *et al.* Massive cell death of immature hematopoietic cells and neurons in Bcl-x-deficient mice. *Science* **267**, 1506–1510 (1995).
18. Ma, A. *et al.* Bclx regulates the survival of double-positive thymocytes. *Proc. Natl Acad. Sci. USA* **92**, 4763–4767 (1995).
19. Lee, P. P. *et al.* A critical role for Dnmt1 and DNA methylation in T cell development, function, and survival. *Immunity* **15**, 763–774 (2001).
20. Rickert, R. C., Roes, J. & Rajewsky, K. B lymphocyte-specific, Cre-mediated mutagenesis in mice. *Nucleic Acids Res.* **25**, 1317–1318 (1997).
21. Godfrey, D. I., Kennedy, J., Suda, T. & Zlotnik, A. A developmental pathway involving four phenotypically and functionally distinct subsets of CD3⁺CD4⁺CD8⁺ triple-negative adult mouse thymocytes defined by CD44 and CD25 expression. *J. Immunol.* **150**, 4244–4252 (1993).
22. Corcoran, A. E., Riddell, A., Krooshoop, D. & Venkataraman, A. R. Impaired immunoglobulin gene rearrangement in mice lacking the IL-7 receptor. *Nature* **391**, 904–907 (1998).
23. Hardy, R. R., Carmack, C. E., Shinton, S. A., Kemp, J. D. & Hayakawa, K. Resolution and characterization of pro-B and pre-pro-B cell stages in normal mouse bone marrow. *J. Exp. Med.* **173**, 1213–1225 (1991).
24. Shinkai, Y. *et al.* RAG-2-deficient mice lack mature lymphocytes owing to inability to initiate V(D)J rearrangement. *Cell* **68**, 855–867 (1992).
25. Kuhn, R., Schwenk, F., Aguet, M. & Rajewsky, K. Inducible gene targeting in mice. *Science* **269**, 1427–1429 (1995).
26. Bouillet, P. *et al.* Proapoptotic Bcl-2 relative Bim required for certain apoptotic responses, leukocyte homeostasis, and to preclude autoimmunity. *Science* **286**, 1735–1738 (1999).
27. Rager, A. M. *et al.* Bad-deficient mice develop diffuse large B cell lymphoma. *Proc. Natl Acad. Sci. USA* **100**, 9324–9329 (2003).
28. Datta, S. R. *et al.* Survival factor-mediated BAD phosphorylation raises the mitochondrial threshold for apoptosis. *Dev. Cell* **3**, 631–643 (2002).
29. Akashi, K., Kondo, M., von Freeden-Jeffry, U., Murray, R. & Weissman, I. L. Bcl-2 rescues T lymphopoiesis in interleukin-7 receptor-deficient mice. *Cell* **89**, 1033–1041 (1997).
30. Maraskovsky, E. *et al.* Bcl-2 can rescue T lymphocyte development in interleukin-7 receptor-deficient mice but not in mutant *rag-1*^{-/-} mice. *Cell* **89**, 1011–1019 (1997).

Supplementary Information accompanies the paper on www.nature.com/nature.

Acknowledgements We thank G. Zambetti for providing the anti-MCL-1 antisera, S. Dowdy for the Tat-Cre, T. Oltersdorf for the GST fusion constructs, J. Fisher and S. Wade for animal husbandry, and E. Smith for editorial assistance. J.T.O. is supported by a postdoctoral fellowship from the Damon Runyon Cancer Research Foundation. This work is supported in part by a grant from the National Institutes of Health.

Competing interests statement The authors declare that they have no competing financial interests.

Correspondence and requests for materials should be addressed to S.K. (stanley_korsmeyer@dfci.harvard.edu).

Optimization of specificity in a cellular protein interaction network by negative selection

Ali Zarrinpar^{1,2}, Sang-Hyun Park² & Wendell A. Lim²

¹Program in Biological Sciences, and ²Department of Cellular and Molecular Pharmacology, University of California, San Francisco, 600 16th Street, San Francisco, California 94143-2240, USA

Most proteins that participate in cellular signalling networks contain modular protein-interaction domains. Multiple versions of such domains are present within a given organism¹: the yeast proteome, for example, contains 27 different Src homology 3 (SH3) domains². This raises the potential problem of cross-

reaction. It is generally thought that isolated domain–ligand pairs lack sufficient information to encode biologically unique interactions, and that specificity is instead encoded by the context in which the interaction pairs are presented^{3,4}. Here we show that an isolated peptide ligand from the yeast protein Pbs2 recognizes its biological partner, the SH3 domain from Sho1, with near-absolute specificity—no other SH3 domain present in the yeast genome cross-reacts with the Pbs2 peptide, *in vivo* or *in vitro*. Such high specificity, however, is not observed in a set of non-yeast SH3 domains, and Pbs2 motif variants that cross-react with other SH3 domains confer a fitness defect, indicating that the Pbs2 motif might have been optimized to minimize interaction with competing domains specifically found in yeast. System-wide negative selection is a subtle but powerful evolutionary mechanism to optimize specificity within an interaction network composed of overlapping recognition elements.

How are SH3 domains used to assemble protein interaction networks with high specificity? One model postulates that domains have diverged sufficiently and have distinct recognition profiles (Fig. 1a). However, peptide library studies have shown that the recognition profiles of SH3 domains are highly overlapping^{5–7}: despite examples of domains with unusual recognition profiles⁸, most bind canonical proline-rich peptide motifs flanked by basic residues on either the amino terminus or the carboxy terminus (for

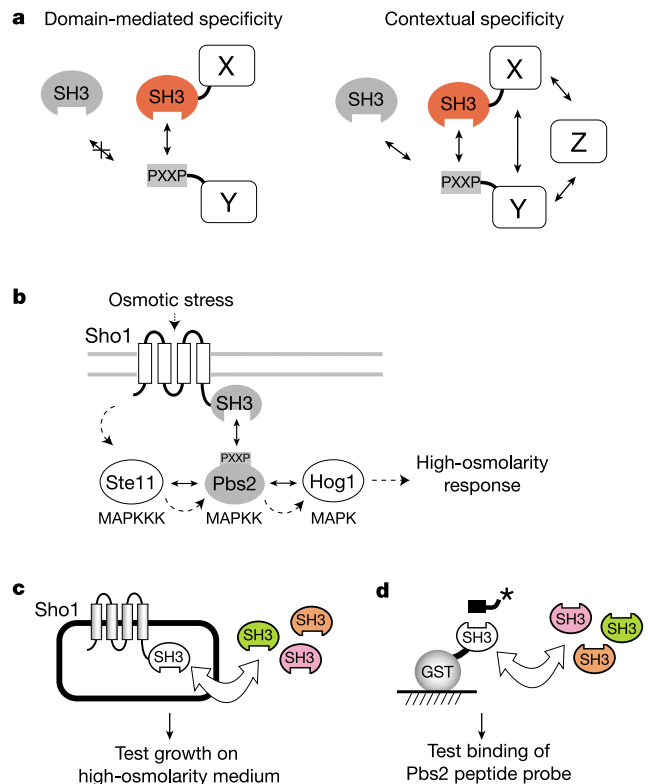


Figure 1 The yeast high-osmolarity pathway as a system for studying SH3 network specificity. **a**, Possible mechanisms of interaction specificity: domain-mediated specificity, in which individual domain–ligand pairs contain enough information to specify unique interactions, and contextual specificity, in which individual domain–ligand pairs lack sufficient information—factors such as cooperative interactions or subcellular localization are required to encode unique interactions. **b**, Interactions in the yeast high-osmolarity response MAP kinase (MAPK) pathway: solid arrows, physical interactions; dashed arrows, activating interactions. **c**, Growth assay to probe SH3 interchangeability *in vivo*: Sho1 chimeras bearing swapped SH3 domains were tested for ability to rescue the osmoresistance of *sho1Δ* strain. **d**, Array assay to test SH3 interchangeability *in vitro*: a set of GST–SH3 fusions arrayed on nitrocellulose were probed for binding to the tagged Pbs2–ligand peptide.

example, R/KXXPPXP or XPXXPXR/K)^{9,10}. It is therefore postulated that specificity *in vivo* is encoded not by isolated domain-peptide partners but rather through the context in which the partners are presented (Fig. 1a)^{3,4}.

To examine the specificity of SH3 domain interactions, we probed the degree to which an SH3 domain from the yeast *Saccharomyces cerevisiae* could be interchanged with other SH3 domains. The fraction of alternative domains that cannot functionally replace the native domain reflects the interaction information content¹¹. If individual domains carry little specificity information, many SH3 domains should be able to act as functional replacements for a native SH3 domain.

The interaction of the SH3 domain from the yeast osmosensor protein Sho1 with a proline-rich motif from the kinase Pbs2 (Fig. 1b) is ideal for studying specificity. First, it is one of the few SH3 domain interactions that are unequivocally biologically relevant: it is essential for signalling in one branch of the high-osmolarity stress response pathway in yeast¹². Second, peptide library screens show that the Sho1 SH3 domain falls within the canonical SH3 recognition class (Supplementary Fig. S1)^{7,13}. Last, there are excellent methods for probing domain function. To probe specificity *in vivo*, we generated Sho1 chimaeras in which the wild-type domain was replaced by alternative SH3 domains (Supplementary Figs S2, S3) and tested their ability to rescue the growth of a Sho1 deletion strain on high-osmolarity media (Fig. 1c). To probe specificity *in vitro*, we made spatially defined arrays of SH3 domains fused to glutathione S-transferase (GST) and assayed these for binding to a labelled Pbs2 ligand (Fig. 1d).

Of 12 metazoan SH3 domains tested, six reconstituted osmo-

resistance when swapped into Sho1 (Fig. 2a). The same six domains bound to the Pbs2 ligand *in vitro* on SH3 domain arrays (Fig. 2b) and in solution binding assays using the free Pbs2 peptide (Fig. 2c). There was a good correlation between binding affinity and ability to rescue function (Supplementary Fig. S4), with a K_d of 40 μ M or less (wild-type $K_d = 1.3 \mu$ M) sufficient to restore detectable pathway function *in vivo*. These results are consistent with low information content in individual SH3 domains: the Pbs2 ligand motif is promiscuously recognized by this set of domains and the native domain is functionally interchangeable.

In contrast, a much higher level of specificity was observed when similar assays were performed with the set of 27 yeast SH3 domains. None of the 26 alternative SH3 domains could reconstitute osmo-resistance (Fig. 2d). This lack of function was not due to changes in expression or localization of chimaeric Sho1 protein (see Supplementary Fig. S5). Moreover, none of the alternative domains tested showed detectable binding to the Pbs2 peptide *in vitro* (Fig. 2e) on the arrays or by solution binding assays (Fig. 2f).

These results suggest that the isolated SH3-domain–ligand pair contains sufficient information to encode interaction specificity among the yeast set of SH3 domains. Several other observations support this model. A non-functional Sho1–SH3 chimaera can be complemented by compensatory changes in the Pbs2 peptide motif (Fig. 2g, Supplementary Fig. S6): the yeast Abp1 SH3 domain reconstitutes function only when combined with Pbs2 bearing an Abp1-binding peptide¹⁴. Moreover, the native interaction pair can be functionally replaced by a heterologous non-SH3 interaction—a PDZ domain interaction¹⁵ (Fig. 2g). Thus, diverse interactions can functionally replace the wild-type SH3-domain–ligand pair, as long

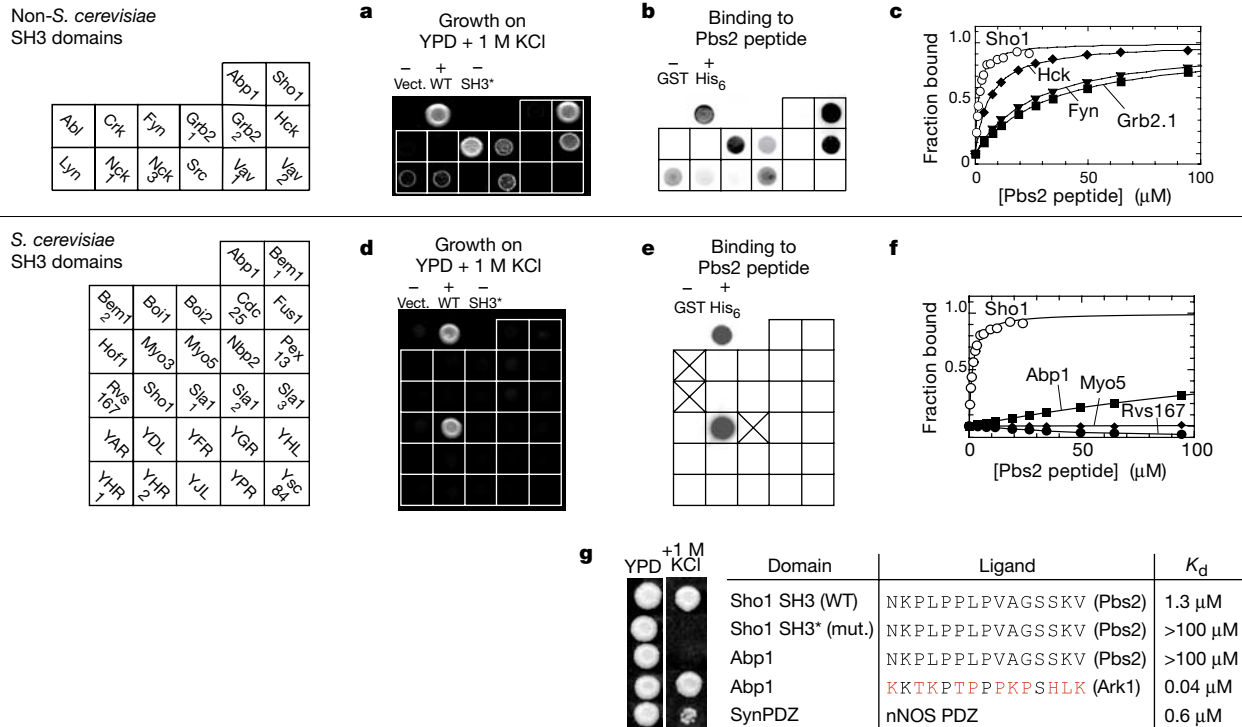


Figure 2 The Sho1 SH3 domain can only be functionally replaced by extra-species (non-*S. cerevisiae*) SH3 domains. **a, d**, Growth of cells containing Sho1 chimaeras (swapped SH3 domains) on high-osmolarity medium. Positive control is wild-type Sho1 (WT); negative controls are vector alone and Sho1 with a non-binding mutation (SH3*: W338F (ref. 30; A.Z., unpublished observations)). The arrangement is shown on the left; subscript indicates domain number in multidomain proteins. **b, e**, SH3 binding arrays. GST–SH3 fusion proteins spotted on nitrocellulose were probed with His-tagged Pbs2 peptide and anti-His antibody. The positive control was a His-tagged protein directly

spotted on membrane; the negative control was GST alone. Positions marked with X indicate insoluble SH3 fusions. **c, f**, Solution binding assays of Pbs2 peptide to representative SH3 domains. **g**, Compensatory changes in Pbs2 ligand can rescue the osmo-resistance of non-functional Sho1 chimaeras. A Pbs2 variant bearing a motif that binds Abp1 SH3 complements a Sho1–Abp1 chimaera. A heterologous PDZ–PDZ-domain interaction pair from syntrophin (Syn) and neuronal nitric oxide synthase (nNOS) can also reconstitute osmo-resistance.

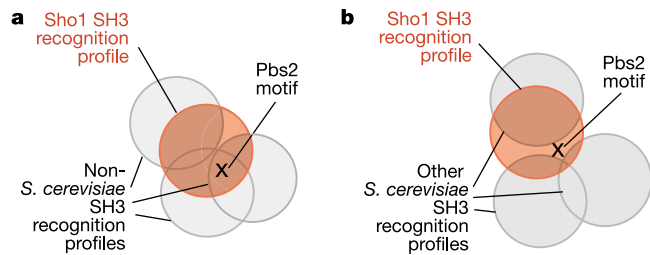


Figure 3 Model: role of proteome-wide negative selection in interaction network specificity. **a**, Non-*S. cerevisiae*: Pbs2 peptide is a canonical motif falling within the recognition space (circles) of several SH3 domains and therefore shows cross-reactivity with many non-yeast SH3 domains. **b**, *S. cerevisiae*: negative selection against cross-reactivity with physiologically relevant competitor domains (that is, other yeast domains) could drive the Pbs2 motif into a sequence space niche compatible only with the Sho1 SH3 domain (red circle).

as the interaction is of sufficient affinity. Other yeast SH3 domains cannot be functionally swapped into Sho1 because they simply do not cross-react with Pbs2.

Why does the interaction between the Sho1 SH3 domain and the Pbs2 ligand show such a high level of specificity within the set of yeast SH3 domains, but not within a set of non-yeast SH3 domains? There is no simple explanation based on sequence clustering of the two SH3 domain sets (Supplementary Figs S2, S3). Instead, an attractive model is that the specificity observed in yeast SH3 domains results not only from positive selection of the Pbs2 ligand

for interaction with the Sho1 SH3 domain, but also from negative selection against binding to competing SH3 domains from the same organism (Fig. 3). If the recognition profile of the Sho1 domain overlaps with those of many other SH3 domains, most random ligands that bind Sho1 will show high levels of cross-reactivity (Fig. 3a). However, if the Pbs2 motif were specifically selected to minimize cross-reaction with other yeast SH3 domains (Fig. 3b), specificity would be observed only within the yeast domain set and not within the non-yeast domain set—only domains within the same proteome would be evolutionarily relevant targets for negative selection. In summary, this model suggests that because interaction domains proliferate over the course of evolution, specificity can be enhanced by a combination of increasing divergence in the domain recognition profiles and pruning of cross-reactivity by negative selection. Binding interactions might be rendered orthogonal through evolution in much the same way that organisms within a single ecosystem speciate to exploit distinct niches¹⁶.

One way of testing the importance of negative selection in interaction network optimization is to probe the sequence space around the Pbs2 motif (Fig. 4a). This model would predict a loss of specificity as the motif drifts away from its optimum. With this aim we made a library of 19 of the 47 possible single-base-pair missense mutations of the Pbs2 motif, leaving the core prolines unchanged (Fig. 4b, Supplementary Fig. S7). We then assayed the specificity and affinity of this ligand library by using yeast SH3 arrays (Fig. 4b). We used the intensity of the Sho1 spot as an index of peptide affinity for the Sho1 domain (Supplementary Fig. S8). As an index of peptide specificity we divided the intensity of the Sho1 spot by the average

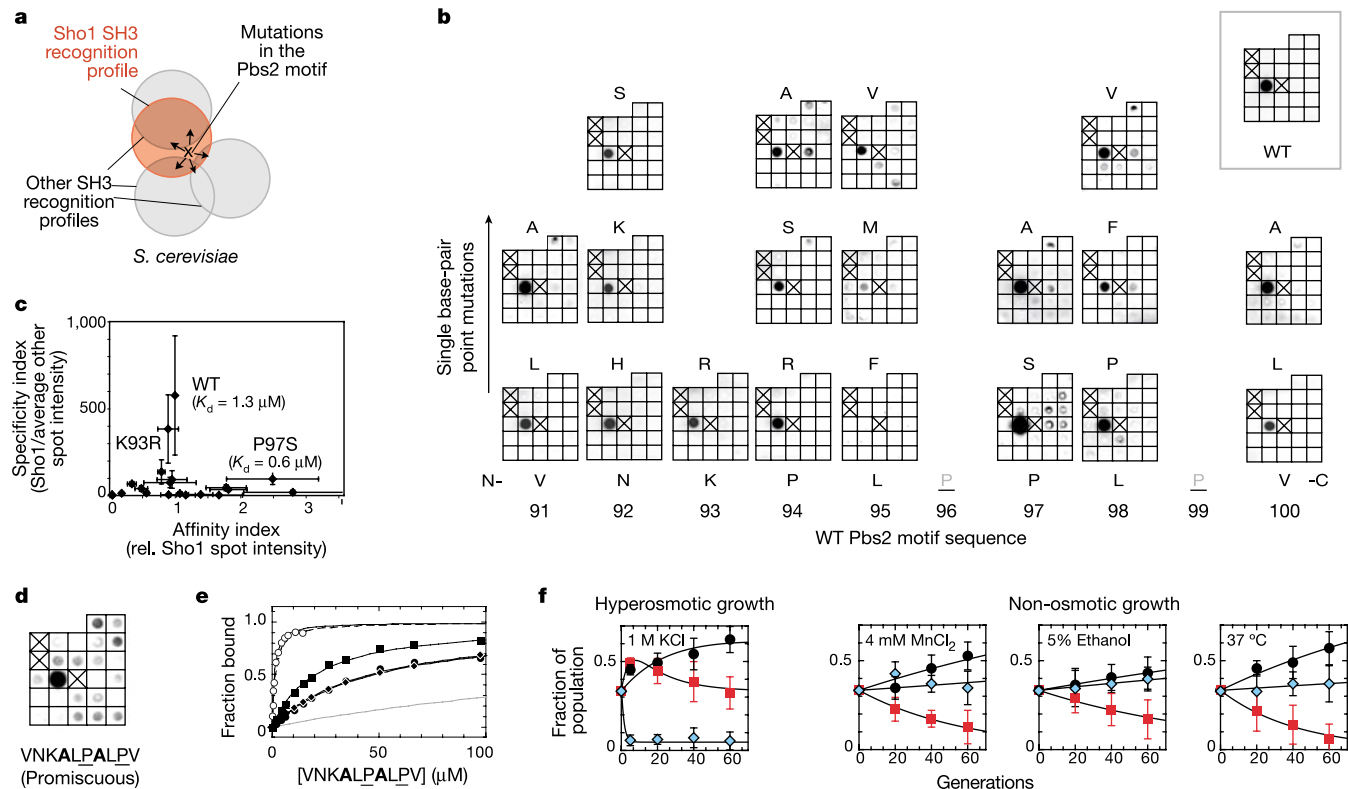


Figure 4 Pbs2 proline-rich motif is optimized to avoid cross-reactivity with other yeast SH3 domains. **a**, Mutational drift of Pbs2 motif is predicted to perturb network negative selectivity in *S. cerevisiae*. **b**, Yeast SH3 domain arrays probed for binding to Pbs2 peptide variants (19 of 47 possible missense point mutants; Supplementary Fig. S7). The wild-type (WT) sequence is shown at the bottom (conserved prolines underlined); point substitutions are indicated above. **c**, Quantification of mutant binding arrays (see Supplementary Fig. S8) shows that the wild-type Pbs2 motif is optimized for Sho1 interaction specificity but not for affinity. **d**, **e**, Combining P94A and P97A mutations yields

a highly promiscuous Pbs2 motif variant, assayed by array binding (**d**) and solution binding assays (**e**). Binding curves of wild-type peptide to Sho1 (dashed line) and Abp1 (grey line) SH3 domains are shown for comparison. Open circles, Sho1; squares, Abp1; filled circles, Rvs167; diamonds, Myo5. **f**, Competition growth assays starting with equal fractions of strains bearing wild-type Pbs2 (VNKLPPLPV; black circles), promiscuous Pbs2 (VNKALPALPV; red squares) and non-interacting Pbs2 (VNKLA~~P~~PLAV; blue diamonds) performed under various conditions.

intensity of the remaining 23 non-Sho1 spots. Some peptide mutations increased affinity, others decreased affinity; but all yielded an increase in cross-reactivity with other yeast SH3 domains (Fig. 4c). On the basis of this mutant analysis, several residues in the ligand seem to be more significant than others in determining specificity. However, it is difficult to rationalize these effects precisely on the basis of structural comparisons (Supplementary Fig. S9).

This analysis indicates that the wild-type Pbs2 motif is not optimized for affinity for the Sho1 SH3 domain. Rather, it seems to be optimized for specificity. In fact, by combining two point mutations (P94A, P97A), we constructed a promiscuous Pbs2 motif variant that bound to the Sho1 SH3 domain with slightly higher affinity than the wild-type Pbs2 motif, but with a markedly higher level of cross-reactivity (Fig. 4d, e). Thus the high specificity of the Sho1–Pbs2 interaction within the yeast SH3 interaction network is not the result of the Sho1 SH3 domain's having a distinct recognition profile; rather, it is the result of the ligand's exploiting niches in sequence space not recognized by other physiologically competitive SH3 domains.

The generation of Pbs2 variants that bind with high affinity to Sho1 but also cross-react significantly with other yeast SH3 domains affords us the opportunity to test the biological importance of interaction network specificity. We compared the fitness of strains containing different forms of Pbs2—wild-type, promiscuous mutant (P94A/P97A) or non-interacting mutant (P96A/P99A, core prolines)—under various growth conditions. Under hyperosmotic growth conditions, the non-interacting mutant strain, because it is osmosensitive, was rapidly overtaken by the other strains. The promiscuous mutant strain, in contrast, was competitive with the wild-type strain. However, under some conditions, such as growth in minimal medium at 37 °C, the promiscuous mutant strain was overtaken by both the wild-type and non-interacting mutant strains (Fig. 4f). Thus, the promiscuous mutant strain seems to have a fitness defect under these conditions that is not due to a defect in the osmolarity response pathway. Promiscuous interactions might lead to small but evolutionarily important disadvantages.

The generality of negative selection as a mechanism for specificity enhancement is difficult to probe because so few biologically verified SH3-domain–ligand pairs in yeast have been clearly identified. Nevertheless, we examined two of the better-characterized yeast SH3 domains, those from Abp1 and Pex13 (Supplementary Fig. S10). A putative ligand for the Abp1 SH3 domain, a peptide from Ark1 (ref. 14), was observed to bind the Abp1 SH3 domain with minimal cross-reactivity against other yeast SH3 domains. In contrast, a proline-rich peptide from Pex14 was found to cross-react with seven other yeast SH3 domains in addition to the Pex13 domain, its native partner¹⁷ (Supplementary Fig. S10). However, previous findings have shown that a functional interaction of Pex13 and Pex14 is dependent on the interaction of both of these proteins with a third protein Pex5 (ref. 18), a case of multi-partner cooperativity in recognition. Moreover, cellular localization studies show that Pex13 is the only SH3-domain-containing protein in peroxisomes^{21,19}. Pex14 also localizes to the peroxisome independently of the Pex13 SH3 domain²⁰. In contrast, Sho1 and Pbs2 both overlap in subcellular localization with up to 16 other SH3-domain-containing proteins^{21,19}. Thus, because of subcellular colocalization and cooperative interactions, the Pex13–Pex14 interaction pair might not have had the same selective pressure to achieve the level of discrimination observed for Sho1–Pbs2. It is also possible that in some cases binding promiscuity is required for function²¹. These results show how negative selection is only one of several possible mechanisms used to enhance interaction specificity.

Thus, negative domain–ligand selection can have a powerful function in optimizing protein interaction network specificity. The power of negative selection has previously been recognized in

immunology²² and is likely to have a key function in the construction of many biological systems, including signalling²³ and transcriptional networks²⁴. The importance of negative selection suggests that to map cellular interaction networks it will be critical not only to search for potential ligands with optimal affinity but also to characterize cross-reactivity of these ligands with relevant sets of competing receptors. In higher eukaryotes, in which only a fraction of a genome is expressed in each cell type^{25,26}, accurate interaction mapping might require the characterization of cell-type-specific domain expression profiles to delineate physiologically competitive domain sets. □

Methods

Constructs and strains

Yeast strains (W303 background) were all derived from the *ssk2Δ,ssk22Δ* mutant, which lacks the Sho1-independent branch of the osmoregulation pathway¹³. Sho1 chimaeras were constructed as shown in Supplementary Fig. S2 and expressed from a CEN/ARS plasmid (pRS316) with the native Sho1 promoter (strain *ssk2Δ,ssk22Δ,sho1Δ* or *ssk2Δ,ssk22Δ,pbs2Δ,sho1Δ*). Pbs2 mutants were constructed in pRS304 with native Pbs2 promoter (Supplementary Fig. S6) and integrated as a single copy into the genome (strain *ssk2Δ,ssk22Δ,pbs2Δ* or *ssk2Δ,ssk22Δ,pbs2Δ,sho1Δ*).

Protein expression and purification

Sho1, Pbs2 and all *S. cerevisiae* SH3 domains were cloned by polymerase chain reaction (PCR) from genomic DNA. Metazoan SH3 domains were cloned from appropriate cDNA libraries. Fragments encoding the SH3 domains were ligated into a Sho1 yeast vector for growth assays (Supplementary Fig. S2) and a GST-fusion vector for bacterial expression. His₆-tagged Pbs2 peptides, fused to the N-terminal domain of lambda repressor (residues 1–99), were constructed as described²⁷ for use as probes for SH3 arrays. Recombinant proteins were expressed in *Escherichia coli* strain BL21 (DE3) RIL. His₆ fusions and GST fusions were purified on Ni²⁺-nitrilotriacetate resin (Qiagen) or glutathione agarose, respectively, by standard methods (elution with 250 mM imidazole or 10 mM glutathione, respectively). Protein concentrations were quantified by ultraviolet radiation absorbance.

Hyperosmotic plate growth assay

Cells (10³) were spotted on YPD plates with or without 1 M KCl (Supplementary Fig. S11). Plates were incubated at 30 °C for 3–5 days.

Peptide synthesis

Peptides (acetylated and amidated) were synthesized with standard 9-fluorenylmethoxycarbonyl (Fmoc) chemistry and purified by reverse-phase chromatography. Molecular masses were verified by mass spectrometry. Concentrations were verified by quantitative amino acid analysis.

SH3 domain array binding assay

100 μl each of 0.1 μM purified GST–SH3 fusion proteins in TBST buffer were spotted in array format on prewetted nitrocellulose membrane with a dot-blot apparatus. Array membranes were blocked in 3% milk, 1% BSA in TBST for 1 h at room temperature, and then probed with 6 ml of the His-tagged fusion protein containing the proline-rich peptide of interest (50 μM) in TBST for 4–16 h at 4 °C. The membrane was washed four times in TBST, then reprobed for 1 h with a horseradish peroxidase-conjugated anti-His6 antibody (dilution 1:2000; Santa Cruz Biotechnology) at 4 °C. Finally, the blot was developed with an enhanced chemiluminescence system and quantified on an AlphaImnotech charge-coupled device camera and analytical software. To control for variation in antibody levels and development exposure, standards of a His-tagged protein (100 μl of 100-nM and 10-nM solutions) were directly spotted on the membrane.

Spot intensities were corrected for background and for variations in spotting and exposure (Supplementary Figs S8a, S11). Corrected intensities for each spot are given relative to the intensity for the Sho1 SH3-domain spot probed with wild-type peptide. The semiquantitative nature of this assay was validated by comparing spot intensities from the SH3-domain arrays with dissociation constants measured *in vitro* (Supplementary Fig. S8b).

Measurement of binding affinities

Affinities of synthetic peptide ligands for SH3 domains were measured by following the increase in domain tryptophan fluorescence on titration of ligand into a solution of SH3 domain at a fixed concentration of 0.01–0.5 μM (always less than 0.25K_d)²⁸. The ligand stock concentration was typically between 0.1 and 2 mM. Data were fitted to the equation

$$y = F_0 + \left[\frac{(F_{\max} - F_0)x}{K_d} \right] / \left[1 + \frac{x}{K_d} \right]$$

by nonlinear least-squares analysis with the program ProFit 5.6.4 (Quantum Soft), where *y* is the fluorescence reading, *x* is ligand concentration, K_d is dissociation constant, F₀ is initial fluorescence value (fraction bound = 0) and F_{max} is fluorescence value at saturation (fraction bound = 1).

Competition growths

Starter cultures of the three strains (Supplementary Fig. S6) were grown independently to an OD₆₀₀ of 0.5. Equal amounts of each were combined into one tube. An aliquot was

removed from this tube as a standard for comparison with subsequent time samples. Cells were diluted 1:100 into various media and incubated at the appropriate temperature until OD_{600} was 0.5, whereupon they were diluted 1:100 (about once or twice a day). Samples were removed at various time points and lysed by incubation with Zymolyase and boiling. The lysates were subjected to PCR. The PCR product was sequenced in accordance with the standard protocol provided by Applied Biosystems and analysed on an ABI Prism 3700 DNA Analyzer with DNA Sequencing Analysis Software Version 3.6.1 (Applied Biosystems, Foster City, California). Mutant frequencies within the culture were estimated with the sequencing-based protocol developed by Kwok and Duan⁹. Data were fitted to exponential equations that accounted for changes in growth of the mutant of interest and changes in growth of competitors.

Received 7 August; accepted 23 October 2003; doi:10.1038/nature02178.

- Pawson, T. & Nash, P. Assembly of cell regulatory systems through protein interaction domains. *Science* **300**, 445–452 (2003).
- Saccharomyces Genome Database, (<http://www.yeastgenome.org/>).
- Mayer, B. J. SH3 domains: complexity in moderation. *J. Cell Sci.* **114**, 1253–1263 (2001).
- Ladbury, J. E. & Arold, S. Searching for specificity in SH domains. *Chem. Biol.* **7**, R3–R8 (2000).
- Sparks, A. B. *et al.* Distinct ligand preferences of Src homology 3 domains from Src, Yes, Abl, Cortactin, p53bp2, PLCgamma, Crk, and Grb2. *Proc. Natl Acad. Sci. USA* **93**, 1540–1544 (1996).
- Kay, B. K., Williamson, M. P. & Sudol, M. The importance of being proline: the interaction of proline-rich motifs in signaling proteins with their cognate domains. *FASEB J.* **14**, 231–241 (2000).
- Cesareni, G., Panni, S., Nardelli, G. & Castagnoli, L. Can we infer peptide recognition specificity mediated by SH3 domains? *FEBS Lett.* **513**, 38–44 (2002).
- Zarrinpar, A., Bhattacharyya, R. P. & Lim, W. A. The structure and function of proline recognition domains. *Science* [online] (doi:10.1126/stke.2003.179.re8).
- Lim, W. A., Richards, F. M. & Fox, R. O. Structural determinants of peptide-binding orientation and of sequence specificity in SH3 domains. *Nature* **372**, 375–379 (1994).
- Feng, S., Chen, J. K., Yu, H., Simon, J. A. & Schreiber, S. L. Two binding orientations for peptides to the Src SH3 domain: development of a general model for SH3–ligand interactions. *Science* **266**, 1241–1247 (1994).
- Schneider, T. D. Evolution of biological information. *Nucleic Acids Res.* **28**, 2794–2799 (2000).
- Posas, F. & Saito, H. Osmotic activation of the HOG MAPK pathway via Ste1p MAPKKK: scaffold role of Pbs2p MAPKK. *Science* **276**, 1702–1705 (1997).
- Tong, A. H. *et al.* A combined experimental and computational strategy to define protein interaction networks for peptide recognition modules. *Science* **295**, 321–324 (2002).
- Fazi, B. *et al.* Unusual binding properties of the SH3 domain of the yeast actin-binding protein Abp1: structural and functional analysis. *J. Biol. Chem.* **277**, 5290–5298 (2002).
- Park, S. H., Zarrinpar, A. & Lim, W. A. Rewiring MAP kinase pathways using alternative scaffold assembly mechanisms. *Science* **299**, 1061–1064 (2003).
- Orr, M. R. & Smith, T. B. Ecology and speciation. *Trends Ecol. Evol.* **13**, 502–506 (1998).
- Barnett, P., Bottger, G., Klein, A. T., Tabak, H. F. & Distel, B. The peroxisomal membrane protein Pex13p shows a novel mode of SH3 interaction. *EMBO J.* **19**, 6382–6391 (2000).
- Bottger, G. *et al.* Saccharomyces cerevisiae PTS1 receptor Pex5p interacts with the SH3 domain of the peroxisomal membrane protein Pex13p in an unconventional, non-PXXP-related manner. *Mol. Biol. Cell* **11**, 3963–3976 (2000).
- Huh, W.-K. *et al.* Global analysis of protein localization in budding yeast. *Nature* **425**, 686–691 (2003).
- Girzalsky, W. *et al.* Involvement of Pex13p in Pex14p localization and peroxisomal targeting signal 2-dependent protein import into peroxisomes. *J. Cell Biol.* **144**, 1151–1162 (1999).
- Sudol, M. From Src Homology domains to other signaling modules: proposal of the 'protein recognition code'. *Oncogene* **17**, 1469–1474 (1998).
- Palmer, E. Negative selection—clearing out the bad apples from the T-cell repertoire. *Nature Rev. Immunol.* **3**, 383–391 (2003).
- Yaffe, M. B. *et al.* A motif-based profile scanning approach for genome-wide prediction of signaling pathways. *Nature Biotechnol.* **19**, 348–353 (2001).
- Newman, J. R. & Keating, A. E. Comprehensive identification of human bZIP interactions with coiled-coil arrays. *Science* **300**, 2097–2101 (2003).
- Kim, S. K. *et al.* A gene expression map for *Caenorhabditis elegans*. *Science* **293**, 2087–2092 (2001).
- Jiang, M. *et al.* Genome-wide analysis of developmental and sex-regulated gene expression profiles in *Caenorhabditis elegans*. *Proc. Natl Acad. Sci. USA* **98**, 218–223 (2001).
- Maxwell, K. L. & Davidson, A. R. Mutagenesis of a buried polar interaction in an SH3 domain: sequence conservation provides the best prediction of stability effects. *Biochemistry* **37**, 16172–16182 (1998).
- Lim, W. A., Fox, R. O. & Richards, F. M. Stability and peptide binding affinity of an SH3 domain from the *Caenorhabditis elegans* signaling protein Sem-5. *Protein Sci.* **3**, 1261–1266 (1994).
- Kwok, P. Y. & Duan, S. SNP discovery by direct DNA sequencing. *Methods Mol. Biol.* **212**, 71–84 (2003).
- Lim, W. A. & Richards, F. M. Critical residues in an SH3 domain from Sem-5 suggest a mechanism for proline-rich peptide recognition. *Nature Struct. Biol.* **1**, 221–225 (1994).

Supplementary Information accompanies the paper on www.nature.com/nature.

Acknowledgements We thank A. Davidson and members of the Davidson laboratory, I. Herskowitz, P. Y. Kwok, E. O'Shea, A. Sali, K. Yamamoto, R. Zuckerman, P. Chien, K. Chak, R. Bhattacharyya, J. Dueber, N. Sallee, B. Yeh, and members of the Lim laboratory for assistance and discussion. This work was supported by grants from the NIH and the Packard Foundation. S.-H.P. is a Jane Coffin Child Fellow. A.Z. is supported by the UCSF Medical Scientist Training Program.

Competing interests statement The authors declare that they have no competing financial interests.

Correspondence and requests for materials should be addressed to W.A.L. (wlim@itsa.ucsf.edu).

Gating of the rapid shade-avoidance response by the circadian clock in plants

Michael G. Salter*, Keara A. Franklin* & Garry C. Whitelam

Department of Biology, University of Leicester, Leicester LE1 7RH, UK

* These authors contributed equally to this work

The phytochromes are a family of plant photoreceptor proteins that control several adaptive developmental strategies^{1,2}. For example, the phytochromes perceive far-red light (wavelengths between 700 and 800 nm) reflected or scattered from the leaves of nearby vegetation. This provides an early warning of potential shading, and triggers a series of 'shade-avoidance' responses, such as a rapid increase in elongation³, by which the plant attempts to overgrow its neighbours³. Other, less immediate, responses include accelerated flowering and early production of seeds. However, little is known about the molecular events that connect light perception with increased growth in shade avoidance. Here we show that the circadian clock gates this rapid shade-avoidance response. It is most apparent around dusk and is accompanied by altered expression of several genes. One of these rapidly responsive genes encodes a basic helix–loop–helix protein, PIL1, previously shown to interact with the clock protein TOC1 (ref. 4). Furthermore PIL1 and TOC1 are both required for the accelerated growth associated with the shade-avoidance response.

Selective absorption of blue and of red (600–700 nm) wavelengths by the chlorophylls means that the radiation reflected/scattered by green leaves is relatively enriched in the far-red (700–800 nm). This far-red-rich light signal (that is, a decrease in the ratio of red to far-red (R/FR)) is detected by nearby plants as a change in the equilibrium between the P_r and P_{fr} forms of phytochromes B, D and E (ref. 5), providing an unambiguous signal that potential competitors are nearby. In response to a low R/FR many plants evoke a suite of adaptive reactions, shade avoidance, including rapidly increased elongation of internodes⁶ and/or petioles, reduced leaf growth and increased apical dominance in an attempt to avoid being shaded. Prolonged exposure to the low-R:FR signal evokes a survival reaction: the acceleration of flowering^{3,7}. Shade avoidance is displayed by most angiosperms, including crop species, conferring high relative fitness in dense stands³ and is one of the best-studied examples of adaptive phenotypic plasticity in plants.

To gain insight into the molecular events involved in rapid shade-avoidance responses, we carried out Affymetrix *Arabidopsis* oligoarray analysis on plants exposed to low R/FR (see Supplementary Information). Among those genes displaying the most marked changes in expression in response to 1 h of low R/FR is the *ATHB-2* gene, encoding a homeodomain ZIP transcription factor; this gene is known to be rapidly and reversibly regulated by changes in R/FR (ref. 8). However, the greatest increase in transcript level in response to low R/FR was observed for a gene annotated as encoding an unknown protein. The transcript of this gene increases in abundance by ~35-fold at 1 h. After correcting for errors in the annotation of this gene, we identified it as *PIL1* (for *PIF3-like 1*) encoding a basic helix–loop–helix protein, previously identified as a protein that interacts with the circadian clock protein TOC1 (ref. 4).

The increase in *PIL1* transcript level in response to low R/FR starting 1 h after dawn is extremely rapid. Quantitative reverse transcriptase polymerase chain reaction (RT-PCR) shows that